JOC Article

Ferrocene-Based Small Molecules for Dual-Channel Sensing of Heavy- and Transition-Metal Cations

Antonio Caballero, Arturo Espinosa, Alberto Tárraga,* and Pedro Molina*

Departamento de Química Orgánica, Facultad de Química, Universidad de Murcia, Campus de Espinardo, E-30100 Murcia, Spain

pmolina@um.es; atarraga@um.es

Received March 31, 2008

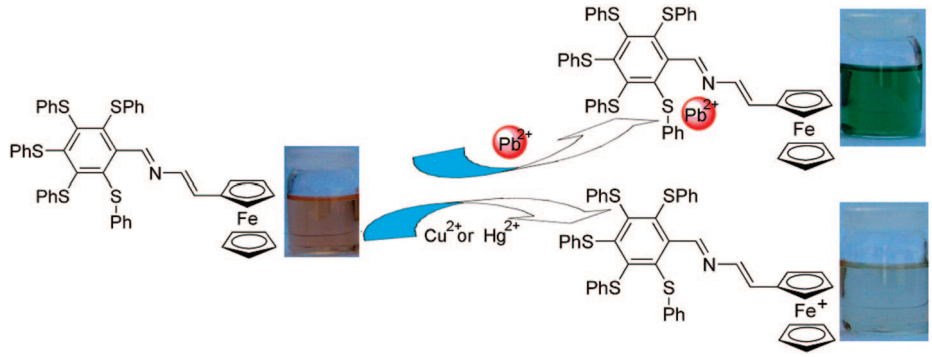

The synthesis, electrochemical, optical, and cation-sensing properties of ferrocene−pentakis(phenylthio)benzene dyads, linked through a putative cation-binding 2-azadiene bridge, are presented. Dyad **5** behaves as a highly selective dual-redox and chromogenic chemosensor molecule for Pb^{2+} cations; the oxidation redox peak is anodically shifted ($\Delta E_{1/2}$ = 125 mV), and the low energy band of the absorption spectrum is red-shifted ($\Delta\lambda$ = 119 nm) upon complexation with this metal cation. Linear sweep voltammetry and spectroelectrochemical studies revealed that Cu^{2+} and Hg^{2+} metal cations induced oxidation of the ferrocene unit. The isomeric dyad **7**, in which the nitrogen atom and the ferrocene unit are in closer proximity, has shown its ability for sensing both Pb^{2+} and Hg^{2+} ions; the oxidation redox peak is anodically higher shifted ($\Delta E_{1/2}$ = 340 mV), and the low energy band of the absorption spectrum is lower red-shifted ($\Delta\lambda$ = 61 nm) that those found for dyad **5**. The changes in the absorption spectra are accompanied by dramatic color changes which allow the potential for "naked eye" detection. A further exciting property of dyad **7** is that it behaves as an electrochemically induced switchable chemosensor for Pb^{2+} and Hg^{2+} because of the low metal-ion affinity of the oxidized $\mathbf{7}^{\bullet+}$ species for these metal cations. The experimental data and conclusions about the ion-sensing properties are supported by DFT calculations.

Introduction

The sensitive detection of heavy and transition-metal ions, such as mercury(II) and lead(II), highly toxic environmental pollutants arising from both natural and industrial sources, is currently a task of prime importance for environmental or biological applications. Mercury, one of the most toxic elements in the world, represents a major toxicity to microorganism and environment even in low concentrations. Inorganic mercury has been reported to produce harmful effects at 5 mg/L in a culture medium.[1] Once introduced into the marine environment, microorganisms convert it into methylmercury, a form of mercury that is even more toxic to aquatic organisms and birds than inorganic mercury, which eventually reaches the top of the food chain and accumulates in higher organisms, especially in large edible fish.[2] When consumed by humans, methylmercury triggers several serious disorders including sensory, motor, and neurological damage.[3] The development of methods for the determination mercury is, therefore, of significant importance for environment and human health. In the past decade, researchers have done a big effort to develop new mercury sensors. An

(1) Boening, D. W. *Chemosphere* **2000**, *40*, 1335–1351.

(2) Krishna, M. V. B.; Ranjit, M.; Karunasagar, D.; Arunachalam, J. *Talanta* **2005**, *67*, 70–80.

(3) Clarkson, T. W.; Magos, L.; Myers, G. J. *N. Engl. J. Med.* **2003**, *349*, 1731–1737.

10.1021/jo800709v CCC: $40.75 © 2008 American Chemical Society
Published on Web 06/18/2008

important number of selective Hg^{2+} chemosensors having been devised using redox,[4] chromogenic,[5] or fluorogenic[6] changes as detection channels.

In the same context, lead pollution is an ongoing danger to the environment[7] and human health, particularly in children (memory loss, irritability, anemia, muscle paralysis, and mental retardation).[8] Thus, the level of this detrimental ion, which is present in tap water as a result of dissolution from household plumbing systems, is the object of several official norms. The World Health Organization established in 1996 guidelines for drinking water quality,[9] which included a lead maximal value of 10 mg L^{-1}. Recently, considerable efforts have been undertaken to develop fluorescent chemosensors for Pb^{2+} ions based on peptide,[10] protein,[11] DNAzyme,[12] polymer,[13] and small-molecule[14] scaffolds.

There is, however, a paucity of use of multichannel receptors as potential guest reporters via multiple signaling patterns. Specifically, the development of multichannel Hg^{2+}- and Pb^{2+}-selective chemosensors is, as far as we know, an unexplored subject, and only few molecule probes have been recently described.[4b,15]

In order to improve both recognition and detection ability of chemosensors for HTM, we turned our attention toward molecular systems combining multiple binding sites and a redox-active signaling unit in one unique molecular material, with the aim of achieving a new type of selective redox and chromogenic molecular sensors. Ferrocene-based ligands have been found to be useful for incorporating redox functions into supramolecular complexes to bind and allow the electrochemical sensing of cations, anions, and neutral molecules by change in the oxidation potential of Fe(II)/Fe(III) redox couple.[16] Due to the special topology of the electron-acceptor group hexakis(phenylthio)benzene (HPTB) and derivatives feature cavities with selective inclusion behavior for several kinds of molecules.[17] With these considerations in mind, we decided to combine the redox activity of the ferrocene group and the binding ability of the HPTB group. Thus, herein we describe the synthesis, electrochemical, and sensing properties of the new ligands **5** and **7** in which a pentakis(phenylthio)phenyl subunit is linked to a ferrocene unit through a 2-aza-1,3-butadiene bridge. The multiresponsive character of the receptors and the ability of the aza-bridge as well as the sulfur-rich aromatic ring to act as favorable binding for cations in the recognition event are most noteworthy.

Results and Discussion

Synthesis. The preparation of the ferrocene derivatives **5** and **7** is outlined in Schemes 1 and 2. Specifically, the isomer **5** bearing the metallocene unit linked to the 4 position of the 2-azadiene bridge was prepared starting from the appropriate N-substituted diethylaminophosphonate **3**, which was obtained in almost quantitative yield by condensation of aminomethylphosphonate **2** with pentakis(phenylthio)benzaldehyde **1**, available from the reaction of pentafluorobenzaldehyde with thiophenyl sodium salt in 1,3-dimethylimidazolidin-2-one.[18] Treatment of **3** with *n*-BuLi at −78 °C and subsequent reaction of the resulting metalloylide with formyl ferrocene **4** provided **5** in 75% yield (Scheme 1).

(4) (a) Jiménez, D.; Martínez-Mañez, R.; Sancenón, F.; Soto, J. *Tetrahedron Lett.* **2004**, *45*, 1257–1259. (b) Caballero, A.; Martínez, R.; Lloveras, V.; Ratera, I.; Vidal-Gancedo, J.; Wurst, K.; Tárraga, A.; Molina, P.; Veciana, J. *J. Am. Chem. Soc.* **2005**, *127*, 15666–15667.

(5) (a) Choi, M. J.; Kim, M. Y.; Chang, S.-K. *Chem. Commun.* **2001**, 1664–1665. (b) Tatay, S.; Gaviña, P.; Coronado, E.; Palomares, E. *Org. Lett.* **2006**, *8*, 3857–3860. (c) Coronado, E.; Galán-Mascarós, J. R.; Martí-Gastaldo, C.; Palomares, E.; Durrant, J. R.; Vilar, R.; Gratzel, M.; Nazeeruddin, Md. K. *J. Am. Chem. Soc.* **2005**, *127*, 12351–12356. (d) Zhang, X.; Shiraishi, Y.; Hirai, T. *Org. Lett.* **2007**, *9*, 5039–5042. (e) Diez-Gil, C.; Caballero, A.; Ratera, I.; Tárraga, A.; Molina, P.; Veciana, J. *Sensors* **2007**, *7*, 3481–3488.

(6) (a) Nolan, E. M.; Lippard, S. J. *J. Am. Chem. Soc.* **2003**, *125*, 14270–14271. (b) Ono, A.; Togashi, H. *Angew. Chem., Int. Ed.* **2004**, *43*, 4300–4302. (c) Guo, X.; Qiuan, X.; Jia, L. *J. Am. Chem. Soc.* **2004**, *126*, 2272–2273. (d) Hennrich, G.; Walther, W.; Resch-Genger, U.; Sonnenschein, H. *Inorg. Chem.* **2001**, *40*, 641–644. (e) Zhang, G.; Zhang, D.; Yin, S.; Yang, X.; Shuai, Z.; Zhu, D. *Chem. Commun.* **2005**, 2161–2163. (f) Wang, J. B.; Qian, X. H. *Org. Lett.* **2006**, *8*, 3721–3724. (g) Zhu, X. J.; Fu, S. T.; Wong, W. K.; Guo, H. P.; Wong, W. Y. *Angew. Chem., Int. Ed.* **2006**, *45*, 3150–3154. (h) Nolan, E. M.; Racine, M. E.; Lippard, S. J. *Inorg. Chem* **2006**, *45*, 2742–2749. (i) Zhao, Y.; Zhong, Z. Q. *Org. Lett.* **2006**, *8*, 4715–4717. (j) Ou, S. J.; Lin, Z. H.; Duan, C, Y.; Zhang, H. T.; Bai, Z. P. *Chem. Commun.* **2006**, 4392–4393. (k) Meng, X. M.; Liu, L.; Hu, H. Y.; Zhu, M. Z.; Wang, M. X.; Shi, J.; Guo, Q. X. *Tetrahedron Lett.* **2006**, *47*, 7961–7964. (l) Ko, S. K.; Yang, Y. K.; Tae, J.; Shin, I. *J. Am. Chem. Soc.* **2006**, *128*, 14150–14155. (m) Che, Y.; Yang, X.; Zang, L. *Chem. Commun.* **2008**, 1413–1415. (n) Díez-Gil, C.; Martinez, R.; Ratera, I.; Tarraga, A.; Molina, P.; Veciana, J. *J. Mater. Chem.* **2008**, *18*, 1997–2002.

(7) Flegal, A. R.; Smith, D. R. *Environ. Res.* **1992**, *58*, 125–133.

(8) Lin-Fu, J. S. Lead Poisoning, A Century of Discovery and Rediscovery. In *Human Lead Exposure*; Needleman, H. L., Ed.; Lewis Publishing: Boca Raton, FL, 1992.

(9) World Health Organization. *Guidelines for Drinking-Water Quality*, 2nd ed.; WHO: Geneva, 1996; Vol. 2, p 940.

(10) Deo, S.; Godwin, H. A. *J. Am. Chem. Soc.* **2000**, *122*, 174–175.

(11) Chen, P.; Greenberg, B.; Taghvi, S.; Romano, C.; van der Lelie, D.; He, C. *Angew. Chem., Int. Ed.* **2005**, *44*, 2715–2719.

(12) (a) Liu, J.; Lu, Y. *J. Am. Chem. Soc.* **2000**, *122*, 10466–10467. (b) Liu, J. Lu, Y. *J. Am. Chem. Soc.* **2003**, *125*, 6642–6643. (c) Liu, J.; Lu, Y. *J. Am. Chem. Soc.* **2004**, *126*, 12298–12305. (d) Chang, I. H.; Tulock, J. J.; Liu, J.; Kim, W.-S.; Cannon, D. M., Jr.; Lu, Y.; Bohn, P. W.; Sweedler, J. V.; Cropek, D. M. *Environ. Sci. Technol.* **2005**, *39*, 3756–376.

(13) Kim, I.-K.; Dunkhorst, A.; Gilbert, J.; Bunz, U. H. F. *Macromolecules* **2005**, *38*, 4560–4562.

(14) (a) Kwon, J. Y.; Jang, Y. J.; Lee, Y. J.; Kim, K. M.; Seo, M. S.; Nam, W.; Yoon, J. *J. Am. Chem. Soc.* **2005**, *127*, 10107–10111. (b) Kavallieratos, K.; Rosenberg, J. M.; Chen, W-Z.; Ren, T. *J. Am. Chem. Soc.* **2005**, *127*, 6514–6515. (c) Lee, J. Y.; Kim, S. K.; Jung, J. H.; Kim, J. S. *J. Org. Chem.* **2005**, *70*, 1463–1466. (d) Liu, J.-M.; Bu, J.-H.; Zheng, Q.-Y.; Chen, C.-F.; Huang, Z.-T. *Tetrahedron Lett.* **2006**, *47*, 1905–1908. (e) Metivier, R.; Leray, I.; Valeur, B. *Chem. Commun.* **2003**, 996–997. (f) Metivier, R.; Leray, I.; Valeur, B. *Chem. Eur. J.* **2004**, *10*, 4480–4490. (g) Chen, C.-T.; Huang, W.-P. *J. Am. Chem. Soc.* **2002**, *124*, 6246–6247. (h) Ma, L.-J.; Liu, Y.-F.; Wu, Y. *Chem. Commun.* **2006**, 2702–2704. (i) Wu, F.-Y.; Bae, S. W.; Hong, J.-I. *Tetrahedron Lett.* **2006**, *47*, 851–8854. (j) He, Q.; Miller, E. W.; Wong, A. P.; Chang, C. J. *J. Am. Chem. Soc.* **2006**, *128*, 9316–9317. (k) Crego-Calama, M.; Reinhoudt, D. N. *Adv. Mater.* **2001**, *13*, 1171–1174. (l) Lee, J. Y.; Kim, S. K.; Jung, J. H.; Kim, J. S. *J. Org. Chem.* **2005**, *70*, 1463–1466.

(15) (a) Martinez, M.; Espinosa, A.; Tárraga, A.; Molina, P. *Org. Lett.* **2005**, *7*, 5869–5872. (b) Xue, H.; Tang, X.-J.; Wu, L.-Z.; Zhang, L.-P.; Tung, C.-H. *J. Org. Chem.* **2005**, *70*, 9727–9734. (c) Lyskawa, J.; Le Derf, F.; Levillain, E.; Mazari, M.; Sallé, M. *Eur. J. Org. Chem.* **2006**, 2322–2328. (d) Remeter, D.; Blanchard, P.; Allain, M.; Grosu, I.; Roncali, J. *J. Org. Chem.* **2007**, *72*, 5285–5290. (e) Zapata, F.; Caballero, A.; Espinosa, A.; Tárraga, A.; Molina, P. *Org. Lett.* **2008**, *10*, 41–44. (f) Yang, H.; Zhou, Z.; Huang, K.; Fu, M.; Li, F.; Yi, T.; Huang, C. *Org. Lett.* **2007**, *9*, 4729–4732. (g) Balandier, J. Y.; Belyasmine, A.; Sallé, M. *Eur. J. Org. Chem.* **2008**, 269–276.

(16) For reviews, see: (a) Beer, P. D.; Gale, P. A.; Chen, Z. *Coord. Chem. Rev.* **1999**, *185−186*, 3–36. (b) Beer, P. D.; Gale, P. A. *Angew. Chem., Int. Ed.* **2001**, *40*, 486–516. (c) Gale, P. A. *Coord. Chem. Rev.* **2001**, *213*, 79–128. For recent examples, see: (d) Otón, F.; Tárraga, A.; Molina, P. *Org. Lett.* **2006**, *8*, 2107–2110. (e) Otón, F.; Tárraga, A.; Espinosa, A.; Velasco, M. D.; Molina, P. *J. Org. Chem.* **2006**, *71*, 4590–4598. (f) Otón, F.; Tárraga, A.; Espinosa, A.; Velasco, M. D.; Molina, P. *Dalton Trans.* **2006**, 3685–3692. (g) Caballero, A.; Lloveras, V.; Curiel, D.; Tárraga, A.; Espinosa, A.; Garcia, R.; Vidal-Gancedo, J.; Rovira, C.; Wurst, K.; Molina, P.; Veciana, J. *Inorg. Chem.* **2007**, *46*, 825–838. (h) Otón, F.; Espinosa, A.; Tárraga, A.; Ramirez de Arellano, C.; Molina, P. *Chem. Eur. J.* **2007**, *13*, 5742–5752.

(17) (a) Hardy, A. D. U.; MacNicol, D. D.; Wilson, D. R. *J. Chem. Soc., Perkin Trans. 2* **1979**, 1011–1019. (b) Pang, L.; Brisse, F.; Lucken, E. A. C. *Can. J. Chem.* **1995**, *73*, 351–361. (c) Michalski, D.; White, M. A.; Bakshi, P. K.; Cameron, T. S.; Swainson, I. *Can. J. Chem.* **1995**, *73*, 513–521. (d) Tucker, J. H. R.; Gingras, M.; Brand, H.; Lehn, J.-M. *J. Chem. Soc. Perkin Trans. 2* **1997**, 1303–1307. (e) Mayor, M.; Lehn, J.-M. *Helv. Chim. Acta* **1997**, *80*, 2277–2285.

(18) Mayor, M.; Büschel, M.; Fromm, K. M.; Lehn, J.-M.; Daub, J. *Chem. Eur. J.* **2001**, *7*, 1266–1272.

SCHEME 1. Synthesis of Receptor 5[a]

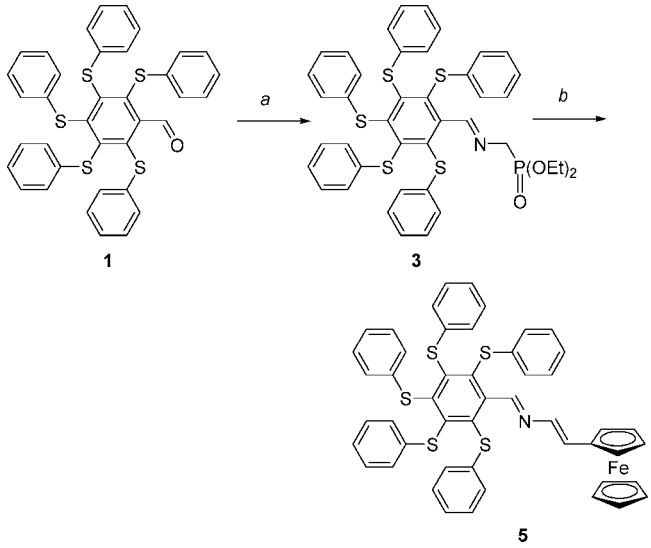

[a] Reagents: (a) diethyl aminomethylphosphonate; (b) (i) *n*-BuLi/−78 °C, (ii) formylferrocene.

SCHEME 2. Synthesis of Receptor 7[a]

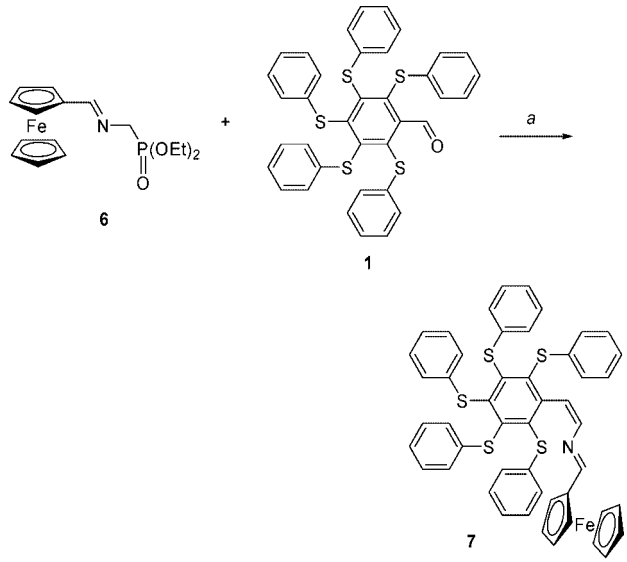

[a] Reagents: (a) *n*-BuLi/−78 °C.

Following the same Horner−Wadsworth−Emmons (HWE) methodology, the isomeric derivative **7** was also prepared. Thus, starting from diethyl [(ferrocenylmethylidene)aminomethyl]phosphonate **6**[19] and **1**, as carbonyl component, the isomer **7**, with the structural feature of having the ferrocene unit linked to the 1 position of the 2-azadiene bridge, was obtained in 67% yield (Scheme 2).

Both 2-aza-1,3-butadiene derivatives **5** and **7** were fully characterized using ^{1}H and ^{13}C NMR and FAB mass spectrometry. In general, the ^{1}H NMR spectra showed the appearance of two pseudotriplets, integrating two protons each, assigned to the four protons within the monosubstituted cyclopentadienyl (Cp) ring and one singlet corresponding to the unsubstituted Cp ring. The protons present in the 2-aza-1,3-butadiene bridge

SCHEME 3. Structure of the Intermediates Formed in the HWE Reaction

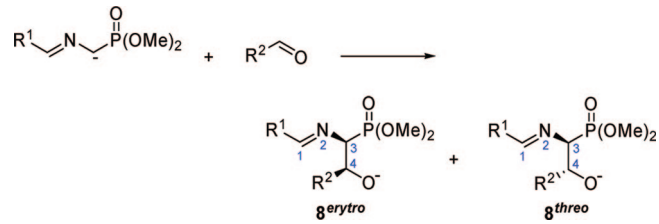

TABLE 1. Calculated[a] Relative Gibbs Free Energies[b] for the Formation of Intermediate Compounds 8 in Model HWE Reactions

	R^1	R^2	erythro	threo
8a	Me	Me	−6.76	−8.79
8b	Ph	Ph	7.84	3.53
8c	Ph	Fc[c]	10.15	6.81
8d	Fc[c]	Ph	4.32	−0.20
8e	$(PhS)_5Ph$	Ph	17.61	14.94
8f	Ph	$(PhS)_5Ph$	15.13	15.74

[a] $CPCM_{(THF)}$/B3LYP/6-311G**//B3LYP/6-31G*. [b] kcal·mol^{-1}. [c] Fc = ferrocenyl.

appeared as one singlet (−C*H*═N−) and two doublets (−C*H*═C*H*−).

Assignment of the configuration of the double bonds present in the 2-aza-1,3-butadiene bridge was achieved by inspection of the corresponding ^{1}H NMR spectroscopic data. It is generally accepted that the stereoselectivity in HWE olefination reactions is a result of both kinetic and thermodynamic control upon the reversible formation of the *erythro* and *threo* adducts and their decomposition to olefins. That is, the stereochemistry is determined by a combination of the stereoselectivity in the initial carbon−carbon bond-forming step and the reversibility of the intermediate adducts. However, in general, this reaction preferentially gives the more stable *E*-disubstituted olefins as a consequence of the predominant formation of the thermodynamically more stable *threo* adducts.[20]

The *E*-configuration of the carbon−carbon double bond in compound **5**, as is expected in this olefination process, was confirmed by the value of the vicinal coupling constants (J = 13.0 Hz). In addition, NOE and two-dimensional NOESY experiments carried out on $CDCl_3$ solutions confirmed the (*E*,*E*)-configuration of the double bonds present in the bridge of this derivative.

By contrast, formation of a carbon−carbon double bond in compound **7**, under the same reaction conditions, takes place with *Z*-stereoselectivity as it was confirmed by analyzing the coupling constants corresponding to the vinyl proton signals (J = 7.80 Hz). In order to explain this unexpected *Z*-selective HWE reaction, a computational study at the DFT level of the intermediate *erythro* and *threo* adducts has been carried out. With the aim of correctly grasping the origin of the *Z*-selectivity, six model HWE reactions have been considered according to Scheme 3. The computed changes in Gibbs free energy for the formation of intermediates $\mathbf{8}^{erythro}$ and $\mathbf{8}^{threo}$ are collected in Table 1.

In the simplest derivative with the smallest substituent, formation of both diastereomeric pairs **8a** is exergonic, with

(19) Lloveras, V.; Caballero, A.; Tárraga, A.; Velasco, M. D.; Espinosa, A.; Wurst, K.; Evans, D. J.; Vidal-Gancedo, J.; Rovira, C.; Molina, P.; Veciana, J. *Eur. J. Inorg. Chem.* **2005**, 2436–2450.

(20) (a) Maryanoff, B. E.; Reitz, A. B. *Chem. Rev.* **1989**, *89*, 863–927, and references cited therein. (b) Ando, K. *J. Org. Chem.* **1997**, *62*, 1934–1939. (c) Ando, K. *J. Org. Chem.* **1998**, *63*, 8411–8416. (d) Wang, Y.; West, F. G. *Synthesis* **2002**, 99–103.

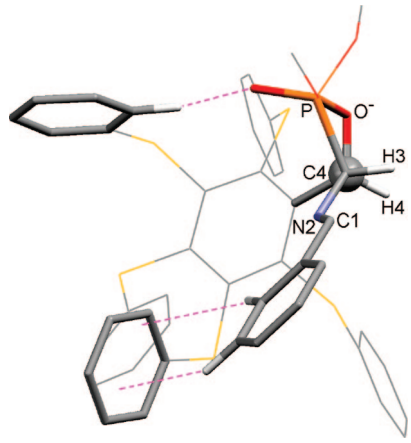

FIGURE 1. Calculated structure for the **8f**^{erythro} intermediate viewed along the axis containing the newly formed C3−C4 bond of the 2-azadiene framework. Unrelevant H atoms are omitted for clarity.

the *threo* pair being more stable than the *erythro* one ($\Delta G^{e/t}_{THF} = -2.03$ kcal·mol^{-1}). A similar tendency ($\Delta G^{e/t}_{THF} = -4.31$ kcal/mol) is observed when two phenyl substituents are present in **8b**, although in this case, formation of both stereoisomers is endergonic. Substitution of the phenyl R^2 group in **8c** or the R^1 by a ferrocenyl unit in **8d**, as in **5** and **7**, respectively, does not alter the above-mentioned higher stabilities of the *threo* over the *erythro* forms ($\Delta G^{e/t}_{THF} = -3.34$ and -4.52 kcal·mol^{-1} for **8c** and **8d**, respectively), in agreement with the experimentally observed *E*-selectivity in the HWE synthesis of several previously reported 1-aryl-4-ferrocenyl-, 4-aryl-1-ferrocenyl-, or even 1,4-diferrocenyl-2-aza-1,3-butadienes[19,21] or their ruthenocenyl analogues.[22] Coming back again to the diphenyl derivative, if the R^1 substituent on the phosphonate component is changed by the more sterically demanding pentakis(phenylthio)phenyl group, the relative difference between the *erythro* and *threo* isomers of **8e** is rougthly maintained ($\Delta G^{e/t}_{THF} = -2.67$ kcal kcal·mol^{-1}), and therefore, the *E*-azadiene is expected to be preferentially formed via the more stable *threo* intermediate. We believe that the same holds true if the phenyl substituent is replaced by a ferrocenyl one, as in the reaction leading to compound **5**. On the contrary, when the bulkiest substituent comes from the carbonyl component, the situation is reversed as far as it is the only case in which the *erythro* intermediate, precursor of the *Z* olefin, is more stable than the *threo* isomer ($\Delta G^{e/t}_{THF} = +0.61$ kcal·mol^{-1}). Again, we assume the same behavior for the intermediates leading to compound **7**. The calculated structure for one of the *erythro* stereoisomers of **8f** is shown in Figure 1, with the numeration as sketched in Scheme 3. The most stable conformation is fixed by one strong hydrogen bridge bond between a phosphonate terminal O atom and an *ortho* H atom ($d_{PO\cdots H} = 2.105$ Å, WBI 0.013; angle O···H−C 158.8°) belonging to a phenylthio group in R^2. The other substituent R^1 is then oriented approaching R^2, whereby an stabilizing aromatic edge-to-face interaction, close to the limiting edge-tilted-T-type,[23] is originated. A similar P−O···H interaction fixes the most stable conformation in the *threo* isomer (see the Supporting Information) but in this case the R^1 substituent is oriented moving away from the bulky R^2 group, therefore lacking the subtle aromatic stabilizing interaction.

Electrochemical and Optical Properties. The redox chemistry of compounds **5** and **7** was investigated by linear sweep voltammetry (LSV), cyclic voltammetry (CV), and Osteryoung square wave voltammetry (OSWV) in a CH_3CN solution containing 0.15 M $[n\text{-}Bu_4N]ClO_4$ (TBAP)[24] as supporting electrolyte. Each receptor exhibited in the range 0−1.0 V a reversible one-electron redox wave, typical of a ferrocene derivative, at the half-wave potential value of $E_{1/2} = 0.590$ V and $E_{1/2} = 0.670$ V versus decamethylferrocene (DMFc), for **5** and **7**, respectively. The criteria applied for reversibility was a separation of 60 mV between cathodic and anodic peaks, a ratio of 1.0 ± 0.1 for the intensities of the cathodic and anodic currents I_c/I_a, and no shift of the half-wave potentials with varying scan rates. From these data, it is clear that the oxidation potentials of the ferrocenyl units are strongly dependent on the position of the 2-azadiene bridge to which they are attached, the oxidation being easier when the ferrocene is linked to the 4 position of the bridge than when it is linked to the 1 position. These derivatives could also show electroactivity due to the presence of the oxidizable 2-aza-1,3-butadiene bridge in their structures. However, upon scanning to higher potential (0−1.5 V), only compound **5** shows a clearly irreversible oxidation wave at $E_{pa} = 1.23$ V vs DMFc, which was attributed to the aza-bridge oxidation, whereas for compound **7** this wave was silent. Moreover, when the voltammetric study was carried out from −2 to +1 V, an additional irreversible wave appeared at $E_{pa} = 1.52$ V and $E_{pa} = 1.31$ V for **5** and **7**, respectively, associated with the reduction process of the pentakis(phenylthio) platform.

The UV−vis data obtained in CH_3CN for compounds **5** and **7** are consistent with most ferrocenyl chromophores in that they exhibit two charge-transfer bands in the UV−vis region.[25] These spectra contain a prominent absorption band with a maximum at 318 nm ($\epsilon = 30340$ M^{-1} cm^{-1}) and 316 nm ($\epsilon = 24100$ M^{-1} cm^{-1}) for **5** and **7**, respectively, which can safely be ascribed to a high energy ligand-centered $\pi-\pi^*$ electronic transition (L−π^*) (HE band). In addition to this band, another weaker absorption is visible at 484 nm ($\epsilon = 2798$ M^{-1} cm^{-1}) and 475 nm ($\epsilon = 1592$ M^{-1} cm^{-1}) for **5** and **7**, respectively, which is assigned to another localized excitation with a lower energy produced either by two nearly degenerate transitions, an Fe(II) d−d transition[26] or by a metal−ligand charge transfer (MLCT) process ($d_\pi-\pi^*$) (LE band). This assignment is in accordance with the latest theoretical treatment (model III) reported by Barlow et al.[27] Such spectral characteristics confer an orange color to these species.

Metal-Ion Sensing Properties. One of the most interesting attributes of ligands **5** and **7** is the presence of a redox-active

(21) (a) Caballero, A.; Tormos, R.; Espinosa, A.; Velasco, M. D.; Tárraga, A.; Miranda, M. A.; Molina, P. *Org. Lett.* **2004**, *6*, 4599–4602. (b) Caballero, A.; Tárraga, A.; Velasco, M. D.; Espinosa, A.; Molina, P. *Org. Lett.* **2005**, *7*, 3171–3174. (c) Caballero, A.; Espinosa, A.; Tárraga, A.; Molina, P. *J. Org. Chem.* **2007**, *72*, 6924–6937. (d) Zapata, F.; Caballero, A.; Espinosa, A.; Tárraga, A.; Molina, P. *Org. Lett.* **2007**, *9*, 2385–2388.

(22) Caballero, A.; García, R.; Espinosa, A.; Tárraga, A.; Molina, P. *J. Org. Chem.* **2007**, *72*, 1161–1173.

(23) (a) Hunter, C. A. *Chem. Soc. Rev.* **1994**, 101–109. (b) Hobza, P.; Selzle, H. L.; Schlag, E. W. *Chem. Rev.* **1994**, *94*, 1767–1785. (c) Hobza, P.; Havlas, Z. *Chem. Rev.* **2000**, *100*, 4253–4264. (d) Jennings, W. B.; Farrell, B. M.; Malone, J. F. *Acc. Chem. Res.* **2001**, *34*, 885–894.

(24) Warning! Perchlorate salts are hazardous because of the possibility of explosion. Only small amounts of this material should be handled and with great caution.

(25) Farrel, T.; Meyer-Friedrichsen, T.; Malessa, M.; Haase, D.; Saak, W.; Asselberghs, I.; Wostyn, K.; Clays, K.; Persoons, A.; Heck, J.; Manning, A. R. *J. Chem. Soc., Dalton Trans.* **2001**, 29–36, and references cited therein.

(26) (a) Sohn, Y. S.; Hendrickson, D. N.; Gray, M. B. *J. Am. Chem. Soc.* **1971**, *93*, 3603–3619. (b) Sanderson, C. T.; Quinian, J. A.; Conover, R. C.; Johnson, M. K.; Murphy, M.; Dluhy, R. A.; Kuntal, C. *Inorg. Chem.* **2005**, *44*, 3283–3289. (c) Gao, L.-B.; Zhang, L.-Y.; Shi, L.-X.; Cheng, Z.-N. *Organometallics* **2005**, *24*, 1678–1684.

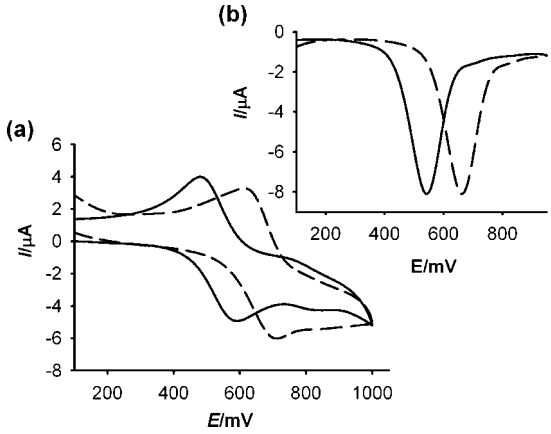

FIGURE 2. Evolution of the CV (a) and OSWV (b) of **5** (1×10^{-3} M) in CH_3CN with TBAP (0.1 M) as supporting electrolyte scanned at 0.1 $V \cdot s^{-1}$ from −0.7 to 1.0 V when $Pb(ClO_4)_2$ is added: from 0 (solid line) to 1 equiv (dashed line). Decamethylferrocene was used as an internal standard.

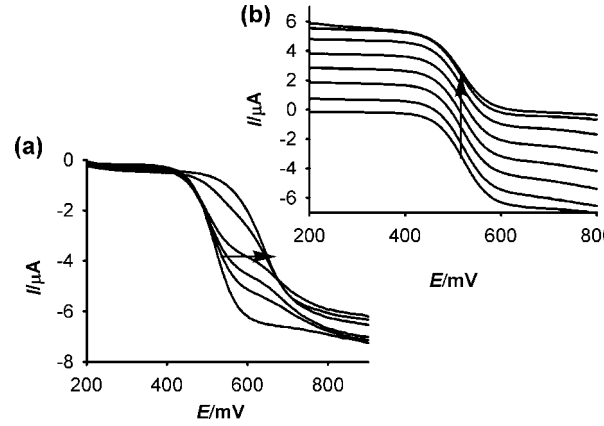

FIGURE 3. Changes in the linear sweep voltammogram of **5** (1×10^{-3} M) in CH_3CN with TBAP (0.1 M) as supporting electrolyte, obtained using a rotating disk electrode at 100 $mV \cdot s^{-1}$ and 1000 rpm, when metal cations are added: (a) upon addition of increasing amounts of Pb^{2+} cations and (b) upon addition of increasing amount of Hg^{2+} cations. Decamethylferrocene was used as an internal standard.

ferrocene moiety close to the cation-binding nitrogen atom within the bridge. Thus, metal recognition properties of these ligands were evaluated by electrochemical, optical, and ^1H NMR techniques.

At first, their electrochemical behavior was investigated in the presence of several metal cations such as Li^+, Na^+, K^+, Ca^{2+}, Mg^{2+}, Cu^{2+}, Zn^{2+}, Cd^{2+}, Hg^{2+}, Ni^{2+}, and Pb^{2+} as their perchlorate salts. Titration studies with addition of the above-mentioned set of metal cations to an electrochemical solution of receptor **5** ($c = 10^{-3}$ M) in CH_3CN containing TBAP (0.1 M) as supporting electrolyte, demonstrate that while addition of Cu^{2+}, Hg^{2+} and Pb^{2+} ions promotes remarkable responses, addition of Li^+, Na^+, K^+, Ca^{2+}, Mg^{2+}, Zn^{2+}, Cd^{2+}, and Ni^{2+} metal ions had no effect either on LSV or on the CV or OSWV of this receptor, even when present in a large excess. The results obtained on the stepwise addition of substoichiometric amounts of Pb^{2+} revealed the appearance, in the OSWV, of a new oxidation peak at a more positive potential ($E_{1/2} = 0.715$ V) ($\Delta E_{1/2} = 0.125$ V) associated with the formation of a complexed species. The current intensity of this new peak increases until 1 equiv of the guest cation is added. At this point, the peak corresponding to the uncomplexed receptor **5** disappears (Figure 2). The positive potential shift ($\Delta E_{1/2} = 0.125$ V) observed for the Fe(II)/Fe(III) redox wave upon complexation by Pb^{2+} cations can be due to electrostatic repulsion effect between the bound metal cation and the electrogenerated positive charge on the oxidized ferrocenyl subunit. This leads to a decrease of the association constant with the oxidized ligand and to a destabilization of the complex. Thus, $\Delta E_{1/2}$ reflects the balance of the interaction of the metal cation between the neutral and the oxidized charged ligand.

Remarkably, LSV studies carried out upon addition of Cu^{2+} and Hg^{2+} to the CH_3CN solution of this ligand showed a significant shift of the sigmoidal voltammetric wave toward cathodic currents, indicating that both metal cations promote the oxidation of the free receptor. By contrast, the same experiments carried out upon addition of Pb^{2+} revealed a shift of the linear sweep voltammogram toward more positive potentials, which is in agreement with the complexation process previously observed by OSWV (Figure 3). Interestingly, addition of Pb^{2+} ions also caused an anodic shift ($\Delta E_{pa} = 202$ mV) in the wave associated to the pentakis(phenylthio) unit (see the Supporting Information).

Similar studies developed using the receptor **7**, under the same electrochemical conditions, demonstrate that while addition of Hg^{2+} and Pb^{2+} ions promotes the formation of the corresponding complexes, addition of Cu^{2+} induces the oxidation of the ferrocene moiety present in this receptor. Moreover, addition of Li^+, Na^+, K^+, Ca^{2+}, Mg^{2+}, Zn^{2+}, Cd^{2+}, and Ni^{2+} metal ions had no effect on the corresponding voltammograms (LSV, DPV or OSWV). In fact, addition of increasing amounts of Hg^{2+} and Pb^{2+} ions caused a progressive disappearance of the oxidation peak present in the free receptor ($E_{1/2} = 0.670$ V) and the simultaneous appearance, in both cases, of a new oxidation wave at $E_{1/2} = 1.010$ V ($\Delta E_{1/2} = 0.340$ V) whose current intensity continuously increases, reaching its maximum when 1 equiv of such metal cations is added (Figure 4). This particular behavior is characteristic of a large equilibrium constant for the binding of this cation by the neutral receptor.[28] Upon addition of Pb^{2+} ions to receptor **7**, a remarkable anodic shift ($\Delta E_{pa} = 215$ mV) in the wave associated to the pentakis(phenylthio) unit was also observed (see the Supporting Information).

This complexation process is also corroborated by using the LSV technique, which showed a gradual positive shift of the Fe(II)/Fe(III) redox couple until the formation of the corresponding complexes is completed. On the other hand, the interaction between ligand **7** and Cu^{2+} ions was also evaluated by LSV, and it was verified that such interaction promotes the oxidation of the free ligand, because upon addition of this metal cation a gradual shift of the linear sweep voltammogran toward cathodic currents was only observed (Figure 5).

Moreover, the CV analysis of the complexes **7**·Hg^{2+} and **7**·Pb^{2+} shows that their reduction processes take place at the same reduction potential showed by the uncomplexed ligand **7**, which is indicative that the complex starts to be disrupted after its electronic oxidation (Figure 4a). This behavior means that

(27) (a) Barlow, S.; Bunting, H. E.; Ringham, C.; Green, J. C.; Bublitz, G. U.; Boxer, S. G.; Perry, J. W.; Marder, S. R. *J. Am. Chem. Soc.* **1999**, *121*, 3715–3723. (b) Yamaguchi, Y.; Ding, W.; Sanderson, C. T.; Borden, M. L.; Morgan, M. J.; Kutal, C. *Coord. Chem. Rev.* **2007**, *251*, 515–524.

(28) (a) Miller, S. R.; Gustowski, D. A.; Chen, Z. H.; Gokel, G. W.; Echegoyen, L.; Kaifer, A. E. *Anal. Chem.* **1988**, *60*, 2021–2024. (b) Medina, J. C.; Goodnow, T. T.; Rojas, M. T.; Atwood, J. L.; Kaifer, A. E.; Gokel, G. K. *J. Am. Chem. Soc.* **1992**, *114*, 10583–10595.

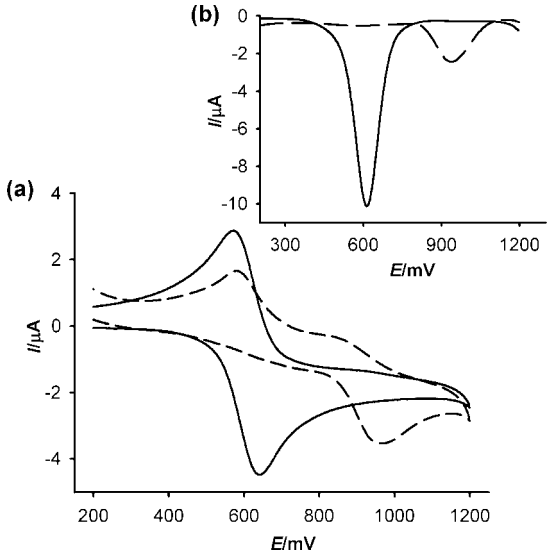

FIGURE 4. Evolution of the CV (a) and OSWV (b) of **7** (1×10^{-3} M) in CH_3CN with TBAP (0.1 M) as supporting electrolyte scanned at 0.1 $V \cdot s^{-1}$ when $Pb(ClO_4)_2$ is added from 0 (solid line) to 1 equiv (dashed line). Decamethylferrocene was used as an internal standard.

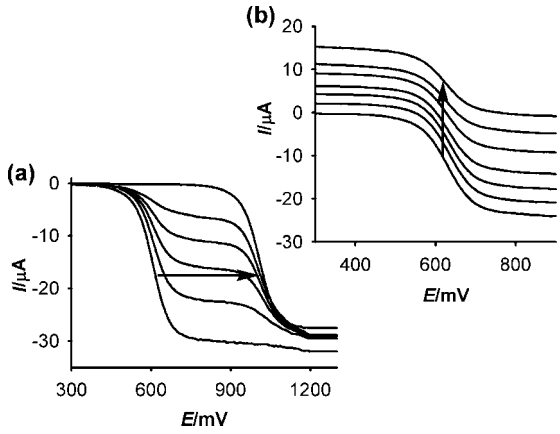

FIGURE 5. Changes in the linear sweep voltammogram of **7** (1×10^{-3} M) in CH_3CN with TBAP (0.1 M) as supporting electrolyte, obtained using a rotating disk electrode at 100 $mV \cdot s^{-1}$ and 1000 rpm, when metal cations are added: (a) upon addition of increasing amounts of Pb^{2+} cations and (b) upon addition of increasing amount of Cu^{2+} cations. Decamethylferrocene was used as an internal standard.

this receptor is not only able to monitor binding but it is also able to behave as an electrochemically induced switchable chemosensor for Pb^{2+} and Hg^{2+} through the progressive electrochemical release of these metal cations; that is, the binding constant upon electrochemical oxidation is decreased.

Previous studies on ferrocene-based ligands have shown that their characteristic low energy (LE) bands in the absorption spectra are perturbed upon complexation.[29] Therefore, the metal recognition properties of the ligands **5** and **7** toward metal ions were also evaluated by UV−vis spectroscopy. Titration experiments for CH_3CN solutions of these ligands ($c = 1 \times 10^{-4}$ M), and the corresponding ions were performed and analyzed

TABLE 2. Relevant UV−vis/Near-IR Data of the Free Receptor, Oxidized Species, and Receptor/Metal Complexes

compd	λ_{max} (nm) (ϵ ($M^{-1}cm^{-1}$))
5	318 (30340), 484 (2798)
5·Pb^{2+}	325 (20660), 356 (sh), 603 (2726)
5·Cu^{2+}	304 (28510), 848 (640)
5·Hg^{2+}	304 (26000), 832 (360)
5$^{\bullet+a}$	304 (28210), 855 (520)
7	316 (24100), 475 (1592)
7·Pb^{2+}	323 (24087), 536 (2653)
7·Cu^{2+}	311 (16435), 819 (125)
7·Hg^{2+}	323 (24100), 536 (2690)
7$^{\bullet+a}$	310 (16500), 852 (123)

[a] Oxidized species obtained electrochemically in CH_2Cl_2 ($c = 1 \times 10^{-3}$ M) using [n-Bu_4N][PF_6] (0.15 M) as supporting electrolyte.

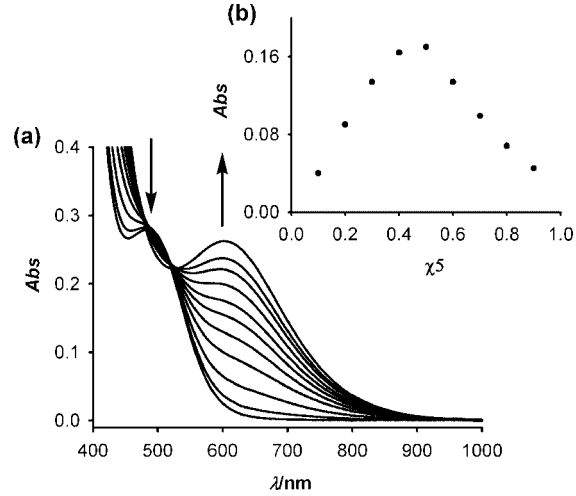

FIGURE 6. (a) Changes in the absorption spectra of **5** (1×10^{-4} M) in CH_3CN upon addition of increasing amounts of Pb^{2+} (2.5×10^{-2} M) in CH_3CN. (b) Job's plot for **5** and Pb^{2+}, indicating the formation of a 1:1 complex. The total [**5**] + [Pb^{2+}] = 1×10^{-4} M (λ_{abs} = 603 nm).

quantitatively.[30] It is worth mentioning that no changes were observed in the UV−vis spectra upon addition of Li^+, Na^+, K^+, Ca^{2+}, Mg^{2+}, Zn^{2+}, Cd^{2+}, and Ni^{2+} metal ions, even in a large excess; however, significant modifications were observed upon addition of Cu^{2+}, Hg^{2+}, and Pb^{2+} (Table 2).

Thus, the addition of increasing amounts of Pb^{2+} ions to a solution of **5** caused the disappearance of the LE band at λ = 484 nm along with a progressive appearance of a new band located at λ = 603 nm (ϵ = 2726 M^{-1} cm^{-1}) as well as a decrease of the initial HE band intensity. Three well-defined isosbestic points at 356, 483, and 519 nm indicate that a neat interconversion between the uncomplexed and complexed species occurs. The new LE band is red-shifted by 119 nm and is responsible for the change of color, from orange to deep green, which can be used for a "naked-eye" detection of this metal ion. Binding assays using the method of continuous variations (Job's plot) (Figure 6) suggests a 1:1 binding model (metal/ligand) with a log $K_a = 4.30 \pm 0.15$.

By contrast, addition of Cu^{2+} and Hg^{2+} metal ions to a solution of **5** produces the same perturbations in its absorption

(29) (a) Marder, S. R.; Perry, J. W.; Tiemann, B. G. *Organometallics* **1991**, *10*, 1896–1901. (b) Coe, B. J.; Jones, C. J.; McCleverty, J. A.; Bloor, D.; Cross, G. J. *J. Organomet. Chem.* **1994**, *464*, 225–232. (c) Müller, T. J.; Netz, A.; Ansorge, M. *Organometallics* **1999**, *18*, 5066–5074. (d) Carr, J. D.; Coles, S. J.; Asan, M. B.; Hurthouse4, M. B.; Malik, K. M. A.; Tucker, J. H. R. *J. Chem. Soc., Dalton Trans.* **1999**, 57–62.

(30) Specfit/32 Global Analysis System, 1999−2004, Spectrum Software Associates (SpecSoft@compuserve.com). The Specfit program was aquired from Bio-logic, SA (www.bio-logic.info) in January 2005. The equation to be adjusted by nonlinear regression using the above-mentioned software was $\Delta A/b = \{K_{11}\Delta\epsilon_{HG}[H]_{tot}[G]\}/\{1 + K_{11}[G]\}$, where H = host, G = guest, HG = complex, ΔA = variation in the absorption, b = cell width, K_{11} = association constant for a 1:1 model, and $\Delta\epsilon_{HG}$ = variation of molar absorptivity.

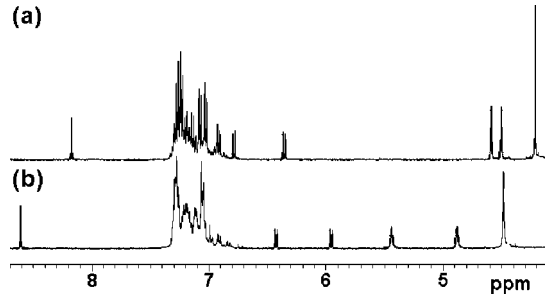

FIGURE 7. ^{1}H NMR spectral changes observed for receptor **7** in CD_3CN (a) and after addition of 1 equiv of Pb^{2+} (b).

spectra as those observed when **5** was electrochemically oxidized (Table 2): a new ligand-to-metal (LMCT) band at $\lambda \approx 800$ nm appears, with concomitant decreasing of the band appearing at $\lambda = 584$ nm.[19]

The stoichiometry of the complex has also been confirmed by ESI-MS, where peaks at *m/z* 1062.3 $[\mathbf{5}\cdot Pb]^{2+}$ and *m/z* 1161.9 $[\mathbf{5}\cdot Pb\cdot(ClO_4)]^+$ are observed. Their relative abundance of the isotopic clusters was in good agreement with the simulated spectrum of the 1:1 complex.

In comparison to the above-mentioned results obtained with ligand **5**, the titration studies of ligand **7** toward the same set of metal cations and under the same conditions revealed a different behavior than **5** upon addition of Cu^{2+}, Hg^{2+}, and Pb^{2+}. In this case, whereas Hg^{2+} and Pb^{2+} promote a clear complexation process, Cu^{2+} induces again the oxidation of the receptor, which is confirmed by comparison of the absorption spectrum resulting from the electrochemical oxidation of **7** and that obtained upon addition of Cu^{2+} metal ions (Table 2). It is worth mentioning that addition of Hg^{2+} and Pb^{2+} elicited the same optical response. In both cases, addition of such divalent metal cations to **7** induced a red shift of the LE band from 475 to 536 nm ($\Delta\lambda = 61$ nm) with simultaneous change in the color of the solution from orange to deep blue. In these cases, 1:1 binding models were also observed and the corresponding binding constants were also determined by the analysis of the spectral titration data by using the already mentioned software (log $K_a = 5.37 \pm 0.21$ for Hg^{2+} and log $K_a = 5.34 \pm 0.18$ for Pb^{2+}).

To support the results obtained by electrochemical and UV−vis experiments, and in order to obtain additional information about the coordination of these metal cations by ligands **5** and **7**, we also performed a ^{1}H NMR spectroscopic analysis. In both cases, the most significant changes observed during the titration experiments are as follows (see the Supporting Information): (1) the iminic proton shifts to downfield: $\Delta\delta = 0.04$ ppm for **5** and $\Delta\delta = 0.27$ ppm for **7**; (2) whereas the two well-separated doublets due to the ethylenic protons, N−C*H*═CH and N−CH═C*H*, within the aza-bridge are clearly upfield-shifted in the case of **7** ($\Delta\delta = -0.67$ ppm and $\Delta\delta = -0.57$ ppm), and in **5** the corresponding protons are slightly upfield ($\Delta\delta = -0.04$ ppm) and downfield ($\Delta\delta = 0.15$ ppm) shifted, respectively; (3) the α- and *β*-protons within the monosubstituted Cp ring of the ferrocene units are downfield shifted: $\Delta\delta_{H\alpha} = 0.08$ and 0.32 and $\Delta\delta_{H\beta} = 0.18$ and 0.11, for **5** and **7**, respectively; (4) the singlet corresponding to the five protons of the unsubstituted Cp ring of the ferrocene moiety is also downshifted in both cases: $\Delta\delta = 0.04$ ppm and $\Delta\delta = 0.11$ ppm for **5** and **7**, respectively (Figure 7). From the magnitude of these observed shifts, it can be surmised that the coordination exerts a more powerful effect on the ligand **7** than in **5**.

For the reported constants to be taken with confidence, we have proved the reversibility of the complexation processes by carrying out the following experimental test: 0.5 equiv of $Pb(ClO_4)_2$ was added to a solution of the receptor **5** in CH_2Cl_2 to obtain the complexed $\mathbf{5}\cdot Pb^{2+}$, whose OSWV voltammogram and UV/vis spectra were recorded. The CH_2Cl_2 solution of the complex was washed several times with water until the color of the solution changed from deep green to orange. The organic layer was dried, and the optical spectrum, DPV voltammogram, and ^{1}H NMR spectrum were recorded and they were found to be the same as that of the free receptor **5**. Afterward, 0.5 equiv of $Pb(ClO_4)_2$ was added to this solution, and the initial UV/vis spectrum, DPV voltammogram, and ^{1}H NMR spectrum of the complex $\mathbf{5}\cdot Pb^{2+}$ were fully recovered together with its deep green color. This experiment was carried out over several cycles, and the optical spectrum was recorded after each step, thus demonstrating the high degree of reversibility of the complexation/decomplexation process (see the Supporting Information). Similar studies were carried out using the receptor **7** and the adequate divalent metal cation (Pb^{2+} and Hg^{2+}), which confirm the reversibility of this process between this receptor and such cationic metal species.

Quantum Chemical Calculations. In order to get information about the coordinating sites of receptors **5** and **7**, DFT-based quantum calculations have also been carried out. First of all, the specific role of the pentakis(phenylthio)phenyl (PPTP) group in the complexation event was separately evaluated by considering the different posibilities of interaction between Hg^{2+} or Pb^{2+} perchlorates and hexakis(phenylthio)benzene (HPTB). In agreement with the X-ray structures obtained for some derivatives,[31] HPTB itself shows a minimum-energy structure featuring a regular alternance of phenylthio groups up and down the central benzene ring, with overall quasi-S_6 symmetry, characterized by dihedral angles of 62.9° and 47.4° around the bonds between the S atoms and the central and terminal aromatic rings, respectively. This pattern in the free receptor forms two cavities whose size is determined by the closest H···H distance of 3.540 Å between inner *ortho* H atoms of the phenyl side arms. The complexation of $M(ClO_4)_2$ salts (M = Pb, Hg) by HPTB occurs with the latter acting as heteroditopic receptor for the $M(ClO_4)^+$ cation and the ClO_4^- anion at every side of the molecule. Formation of the corresponding $(ClO_4)\cdot HPTB\cdot M(ClO_4)$ complexes resulted from slightly endergonic processes in both cases ($\Delta G°_{compl} = 8.79$ and 10.40 kcal·mol^{-1} for M = Pb and Hg, respectively) (see below) under the working level of theory. Binding of a $Pb(ClO_4)^+$ cation by HPTB is slightly exergonic ($\Delta G°_{compl} = -2.65$ kcal·mol^{-1}) and preorganizes the other half of the receptor for hosting a ClO_4^- anion with very little modification ($L_{strain} = 0.51$ kcal·mol^{-1}). Conversely, complexation by HPTB of a $Hg(ClO_4)^+$ unit has been found to be highly unstable ($\Delta G°_{compl} = 64.27$ kcal·mol^{-1}), and instead, separated interaction with Hg^{2+} and ClO_4^- ions is preferred ($\Delta G°_{compl} = 26.86$ kcal·mol^{-1}) although still considerably endergonic.

Among several local minima, the lowest energy geometries for the compounds derived from the complexation of azadienes **5** and **7** with $M(ClO_4)_2$ salts (M = Pb, Hg) were those obtained from the above $(ClO_4)\cdot HPTB\cdot M(ClO_4)$ complexes upon substitution of one phenylthio sidearm by the appropriate ferrocenyl-

(31) (a) MacNicol, D. D.; Wilson, D. R. *J. Chem. Soc., Chem. Commun.* **1976**, 494. (b) MacNicol, D. D. In *Inclusion Compounds*; Atwood, J. L., Davies, J. E. D., MacNicol, D. D., Eds.; Academic Press: London, 1984; Vol. 2, Chapter 5.

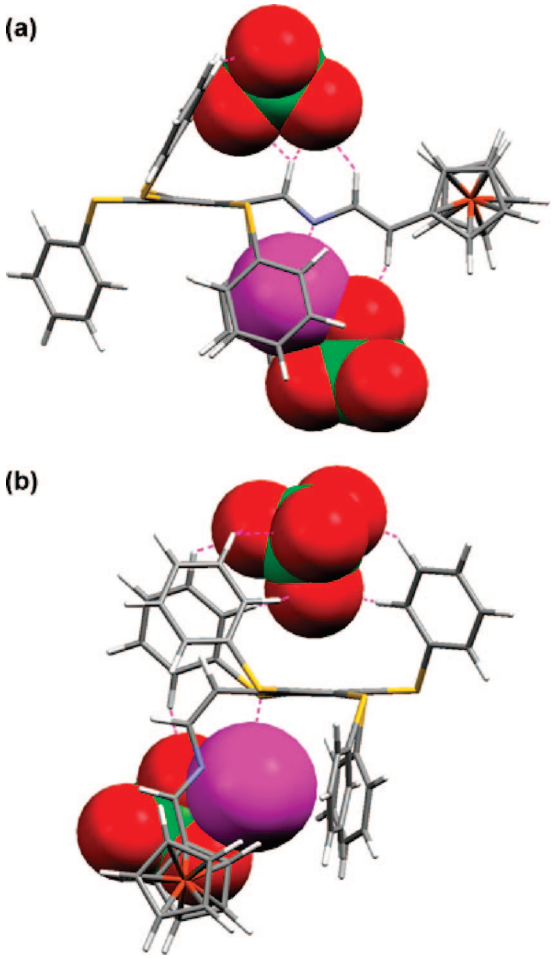

FIGURE 8. (a) Calculated structure for complex **5**·Pb(ClO$_4$)$_2$. Host in capped sticks and guest highlighted in space-filling representation. (b) Calculated structure for complex **7**·Pb(ClO$_4$)$_2$. Host in capped sticks and guest highlighted in space-filling representation.

azadiene moiety. Thus, in **5**·Pb(ClO$_4$)$_2$ (Figure 8a) the coordination sphere around Pb^{2+} is completed by coordination with the azadiene N atom ($d_{N\cdots Pb}$ = 2.463 Å, WBI 0.242) and two phenyl rings that are positioned in virtually parallel planes at both sides of the azadiene bidge (closest $d_{C\cdots Pb}$ = 3.058 and 3.098 Å, total WBI_{Ph-Pb} 0.173 and 0.166). The second perchlorate unit is located at the other side of the PPTP group and interacting via hydrogen bridge bonds with H1 and H3 of the 2-azadiene bridge.

As expected, according to our calculations the complex resulting from the reaction of **5** with Hg(ClO$_4$)$_2$ had a geometry corresponding to the oxidized receptor $\mathbf{5}^{\cdot+}$ interacting with the reduced Hg(I) perchlorate, as evidenced by the electronic and structural features collected in Table 3, which nicely agree with the above-mentioned experimental results. Specially relevant is the total natural charge within the ferrocenyl unit, very much higher than the residual values obtained for **5** or its complex with Pb(ClO$_4$)$_2$. Furthermore we have recently found[19] that the distance between Fe atom and the centroid of the cyclopentadienyl rings has diagnostig relevance for characterizing the oxidation degree in ferrocene or ruthenocene derivatives, as far as it results almost insensitive to the nature of electron donating or withrawing substituents but is considerably increased in radical-cation metallocinium species, probably because of the removal of an electron which is slightly bonding with respect to the metal-ring interaction. The large calculated complexation

TABLE 3. Selected Electronic, Structural, and Thermodynamic Parameters for the Calculated Structures of Receptors 5 and 7 and Their Complexes with Pb(ClO$_4$)$_2$ and Hg(ClO$_4$)$_2$

	Q_{Fc}[a]	d_{Fe-Cpb}[b]	ΔG_{compl}[c]	L_{strain}[c]
$FcH^{\cdot+}$	0.745	2.27		
5	0.008	0.17		
5·Pb(ClO$_4$)$_2$	0.068	0.52	1.66	11.71
5·Hg(ClO$_4$)$_2$	0.847	6.50	−48.90	18.24
7	0.051	0.25		
7·Pb(ClO$_4$)$_2$	0.141	0.99	−2.85	7.76
7·Hg(ClO$_4$)$_2$	0.141	1.00	−15.63	6.36

[a] Total natural charge (au) along the ferrocenyl unit. [b] Distance between Fe and Cp centroid for the unsubstituted ring (Cp_b), referenced to that calculated for parent ferrocene, 1.654 Å (Å × 10^{-2}). [c] Free energies in CH_3CN solution (kcal·mol^{-1}).

energy is mainly due to the internal redox process, as evidenced by the analogous reaction in the model system HPTB, as far as the initial formation of (ClO$_4$)·HPTB·Hg(ClO$_4$) is endergonic (see before) but in the presence of ferrocene the intermolecular redox process to give HPTB·Hg(ClO$_4$) and FcH·(ClO$_4$) is considerably exergonic (ΔG°_{redox} = −50.11 kcal·mol^{-1}).

For receptor **7** calculations predict the same behavior for both metal diperchlorates and internal redox processes were observed in no case (Table 3), in agreement with the experimental evidence. In the complex **7**·Pb(ClO$_4$)$_2$ (Figure 8b), the Pb(ClO$_4$)$^+$ unit is located so as to allow the Pb^{2+} cation to complete its coordination sphere with the N atom of the azadiene bridge ($d_{N\cdots Pb}$ = 2.530 Å, WBI 0.229) one S atom at the PPTP group ($d_{S\cdots Pb}$ = 2.909 Å, WBI 0.339) and a phenyl substituent (closest $d_{C\cdots Pb}$ = 3.521 Å, total WBI_{Ph-Pb} 0.084). Again, the second perchlorate unit is located at the other side of the PPTP group and interacting with the *ortho* and *meta* H atoms of three phenyl groups. The structure of **7**·Hg(ClO$_4$)$_2$ (see the Supporting Information) very much resembles that of Pb^{2+}, with analogous bonding of Hg^{2+} to N ($d_{N\cdots Hg}$ = 2.492 Å, WBI 0.035), S ($d_{S\cdots Hg}$ = 2.496 Å, WBI 0.117), and phenyl (closest $d_{C\cdots Hg}$ = 3.020 Å, total WBI_{Ph-Hg} 0.020) donors.

Conclusion

The synthesis, electrochemical, optical, and cation sensing properties of ferrocene−pentakis(phenylthio)benzene dyads, linked through a putative cation binding 2-azadiene bridge, are presented. The synthetic methodology for the preparation of the 1,4-disubstituted 2-aza-1,3-butadienes **5** and **7** is based on the temporal condensation of the readily available aminomethylphosphonate with the appropriate aldehyde followed by metalation of the resulting phosphonate and subsequent reaction with a different aldehyde. The substituent at position 1 arises from the aldehyde used in the first step, whereas the substituent at position 4 comes from the aldehyde used in the last step. The binding events are strongly affected by the relative position of the ferrocene with respect the nitrogen atom, indicating that shorter distances between the nitrogen donor atom within the bridge and the ferrocene unit correspond to smaller selectivity in the recognition properties of the ligand. Dyad **5** behaves as a highly selective dual redox and chromogenic chemosensor for Pb^{2+} cations; the oxidation redox peak is anodically shifted ($\Delta E_{1/2}$ = 125 mV) and its low-energy band of the absorption spectrum is red-shifted ($\Delta\lambda$ = 119 nm), upon complexation with this metal cation. Whereas, Cu^{2+} and Hg^{2+} metal cations induced oxidation of the ferrocenyl-end group, which is confirmed by spectroelectrochemical studies and linear sweep

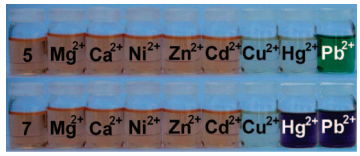

FIGURE 9. Changes in the color of ligand **5** (up) and **7** (down) upon addition of the corresponding cation.

voltammetric (LSV) data. The isomeric dyad **7**, in which the nitrogen atom and the ferrocene unit are in closer proximity, displays the same type of sensing properties toward Pb^{2+} and Hg^{2+} ions; the oxidation redox peak is higher anodically shifted ($\Delta E_{1/2} = 340$ mV), and the low energy band of the absorption spectrum is lower red-shifted ($\Delta\lambda = 61$ nm) than those found for dyad **5**, whereas Cu^{2+} cations promote the oxidation of the ferrocene unit. The changes in the absorption spectra are accompanied by dramatic color changes, from orange to deep green for receptor **5** and orange to deep blue for receptor **7**, which allow the potential for "naked eye" detection (Figure 9). Moreover, dyad **7** also exhibited a selective Pb^{2+} and Hg^{2+} redox induced complexation/decomplexation type of signaling patterns that can be used for the construction of more elaborate supramolecular switching systems.

Experimental Section

Diethyl *N*-[Pentakis(phenylthio)]benzylidenaminomethylphosphonate, 3. To a mixture of diethyl aminomethylphosphonate (0.157 g, 0.93 mmol) and anhydrous Na_2SO_4 (10 g) in dry CH_2Cl_2 (30 mL) was added dropwise an equimolecular amount of pentakis(phenylthio)benzaldehyde **1** in CH_2Cl_2 (10 mL). The resulting solution was stirred at room temperature for 2 h and then filtered. From the filtrate, the solvent was removed under vacuum to give the corresponding aminomethylphosphonate **3** in almost quantitative yield, as a colorless oil which was used, without further purification, in the next step. ^{1}H NMR (400 MHz, $CDCl_3$): δ 1.14 (t, 6H, $^4J_{H,P}$ = 7.2 Hz), 3.72 (d, 2H, $^2J_{H,P}$ = 15.9 Hz), 3.94−3.99 (m, 4H), 6.82−7.10 (m, 25H), 7.97 (d, 1H,$^4J_{H,P}$ = 4.5 Hz). ^{13}C NMR (100 MHz, $CDCl_3$): δ 16.3 (d, $^3J_{P,C}$ = 5.9 Hz), 56.9 (d, $^1J_{P,C}$ = 154.3 Hz), 62.2 (d, $^2J_{P,C}$ = 6.5 Hz), 126.0, 126.3, 128.1, 128.2, 128.2, 128.4, 128.7, 128.8, 129.0, 137.2, 137.4, 137.6, 141.8, 146.4, 147.5, 149.1, 164.2 (d, $^3J_{P,C}$ = 18.3 Hz). ^{31}P NMR (162.29 MHz, $CDCl_3$): δ 22.09. FAB MS: *m*/*z* (relative intensity): 796 (100, $M^+ + 1$).

General Procedure for the Preparation of 1,4-Disubstituted 2-Aza-1,3-butadienes 5 and 7. To a solution of the appropriate N-substituted diethyl aminomethylphosphonate **3** or **6** (1.0 mmol) in dry THF (15 mL) at −78 °C and under nitrogen atmosphere was added *n*-BuLi 1.6 M in hexane (0.33 mL). Then, a solution of the adequate aldehyde (1.0 mmol) in dry THF (10 mL) was slowly added, and the mixture was stirred for 1.5 h. The reaction mixture was allowed to reach the room temperature (30 min), and then it was heated under reflux temperature overnight. After the solution was cooled at 0 °C for 30 min, a precipitate was formed which was filtered and washed with diethyl ether (2 × 10 mL) to give the corresponding 1,4-disubstituted 2-aza-1,3-butadiene, which was recrystallized from THF.

2-Aza-4-ferrocenyl-1-[pentakis(phenylthio)phenyl]-1,3-butadiene 5. Yield: 75%. Mp: 165−166 °C. ^{1}H NMR (400 MHz, $CDCl_3$): δ 4.20 (s, 5H), 4.33 (st, 2H), 4.40 (st, 2H), 6.90 (d, 1H, J = 13.0 Hz), 6.91 (d, 1H, J = 13.0 Hz,), 7.21−7.44 (m, 25H), 8.14 (s, 1H). ^{13}C NMR (100 MHz, $CDCl_3$): δ 67.3 (2 × CH), 69.4 (5 × CH), 69.5 (2 × CH), 80.8, 126.0, 126.1, 126.4, 128.0, 128.3, 128.7, 128.8, 128.9, 129.1, 131.5, 137.3, 137.6, 137.8, 138.3, 143.0, 146.0, 146.8, 148.8, 156.8. FAB MS: *m*/*z* (relative intensity): 856 (100, $M^+ + 1$). Anal. Calcd for $C_{49}H_{37}FeNS_5$: C, 68.75; H, 4.36; N, 1.64. Found: C, 68.60; H, 4.26; N, 1.75.

2-Aza-1-ferrocenyl-4-[pentakis(phenylthio)phenyl]-1,3-butadiene 7. Yield: 67%. Mp: 60−61 °C. ^{1}H NMR (400 MHz, $CDCl_3$): δ 4.18 (s, 5H), 4.47 (st, 2H), 4.56 (st, 2H), 6.63 (d, 1H, J = 7.8 Hz), 6.89 (d, 1H, J = 7.8 Hz,), 6.69−7.07 (m, 25H), 8.15 (s, 1H). ^{13}C NMR (100 MHz, $CDCl_3$): δ 69.1 (2 × CH), 69.5 (5 × CH), 71.1 (2 × CH), 81.1, 123.2, 125.4, 125.6, 126.0, 127.3, 127.5, 127.6, 127.7, 128.0, 128.6, 128.6, 138.4, 142.3, 144.1, 147.6, 148.9, 163.1. FAB MS: *m*/*z* (relative intensity): 856 (100, $M^+ + 1$). Anal. Calcd for $C_{49}H_{37}FeNS_5$: C, 68.75; H, 4.36; N, 1.64. Found: C, 68.87; H, 4.20; N, 1.80.

Acknowledgment. We gratefully acknowledge the financial support from Fundación Séneca (Agencia de Ciencia y Tecnología de la Región de Murcia) projects 02970/PI/05 and 04509/GERM/06 (Programa de Ayudas a Grupos de Excelencia de la Región de Murcia, Plan Regional de Ciencia y Tecnología 2007/2010). A.C. also thanks to Ministerio de Educación y Ciencia a predoctoral grant.

Supporting Information Available: General comments; computational details; NMR spectra, electrochemical, UV−vis, and ^{1}H NMR titration experiments; reversibility experiments; DFT-calculated structures. This material is available free of charge via the Internet at http://pubs.acs.org.

JO800709V